

Lecture 13 Damped, Driven and Nonlinear Oscillators (See Chapters 1 and 2 in B&G)

No discussion of classical mechanics is complete without a review of damped, driven oscillators. Consider first the equation of motion for a linear (viscous) damped oscillator,

$$m\ddot{x} + \gamma\dot{x} + kx = 0. \quad (13.1)$$

We scale out the mass and define new constants

$$\ddot{x} + 2\lambda\dot{x} + \omega_0^2 x = 0, \quad \lambda = \frac{\gamma}{2m}, \quad \omega_0^2 = \frac{k}{m}. \quad (13.2)$$

As usual for a linear equation we try an Ansatz based on an exponential,  $x(t) = Ae^{-\beta t}$  (in case  $\beta$  develops an imaginary part the initial conditions will force us to take the real part in the end) to find

$$\begin{aligned} & [\beta^2 - 2\beta\lambda + \omega_0^2] Ae^{-\beta t} = 0 \\ \Rightarrow \beta = \lambda \pm \sqrt{\lambda^2 - \omega_0^2} = & \begin{cases} \lambda \pm i\sqrt{\omega_0^2 - \lambda^2}, \lambda < \omega_0 \text{ [damped]} \\ \lambda, \lambda = \omega_0 \text{ [critically damped]} \\ \lambda \pm \sqrt{\lambda^2 - \omega_0^2}, \lambda > \omega_0 \text{ [over damped]} \end{cases}. \end{aligned} \quad (13.3)$$

In the usual (just) damped case, assuming a real coordinate  $x$ , we have

$$x(t) = e^{-\lambda t} A \cos[\omega_\lambda t + \phi], \quad \omega_\lambda = \sqrt{\omega_0^2 - \lambda^2}. \quad (13.4)$$

The motion is a damped oscillation with a frequency smaller than the natural frequency,  $\omega_\lambda < \omega_0$ . In the other cases we observe just damped motion, perhaps with an extra factor of  $t$  in the critically damped case ( $x(t) = e^{-\lambda t} (A + Bt)$ ). The constants  $A$  and  $\phi$  are determined by the initial conditions.

Now consider a driven oscillator where we can, without loss of generality, assume that the driving force can be written as a sum of sinusoidal terms. Since we have a linear equation of motion (for the moment) where superposition holds, we need only solve the driven problem for one frequency. We can always sum up the results later

if the Fourier expansion of the force requires several terms of different frequencies. Consider the form

$$\begin{aligned}
 m\ddot{x} + \gamma\dot{x} + kx &= f \cos(\omega_D t) \\
 \Rightarrow \ddot{x} + 2\lambda\dot{x} + \omega_0^2 x &= \frac{f}{m} \cos(\omega_D t).
 \end{aligned}
 \tag{13.5}$$

The general solution will be the sum of the homogenous solution of Eq. (13.4) plus a particular solution. For the latter we take a complex exponential form matching the time dependence of the driving force, *i.e.*, take the driving force to have the corresponding complex form and write

$$\begin{aligned}
 x_p(t) &= \text{Re } B e^{i\omega_D t} \\
 \Rightarrow [-\omega_D^2 + 2i\omega_D\lambda + \omega_0^2] B e^{i\omega_D t} &= \frac{f}{m} e^{i\omega_D t} \\
 \Rightarrow B &= \frac{f}{m} \frac{1}{\omega_0^2 + 2i\omega_D\lambda - \omega_D^2}.
 \end{aligned}
 \tag{13.6}$$

If we define  $\varphi$  to be the phase of  $B$ , we have

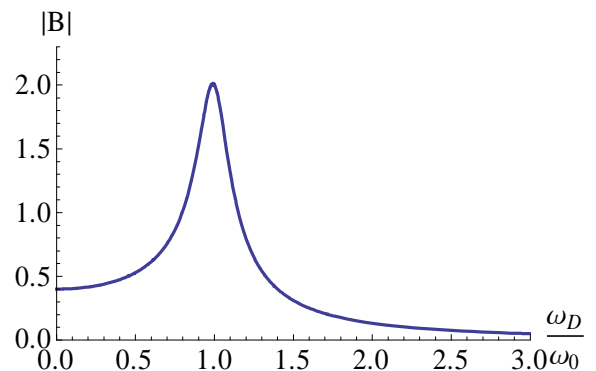
$$\begin{aligned}
 \varphi &= \tan^{-1} \left( \frac{-2\lambda\omega_D}{\omega_0^2 - \omega_D^2} \right), \\
 B &= \frac{f}{m} \frac{e^{i\varphi}}{\sqrt{(\omega_0^2 - \omega_D^2)^2 + (2\omega_D\lambda)^2}}, \\
 x_p(t) &= \frac{f}{m} \frac{\cos(\omega_D t + \varphi)}{\sqrt{(\omega_0^2 - \omega_D^2)^2 + (2\omega_D\lambda)^2}} \\
 \Rightarrow x(t) &= e^{-\lambda t} A \cos[\omega_\lambda t + \phi] + \frac{f}{m} \frac{\cos(\omega_D t + \varphi)}{\sqrt{(\omega_0^2 - \omega_D^2)^2 + (2\omega_D\lambda)^2}}.
 \end{aligned}
 \tag{13.7}$$

(Note that this result involves two phases,  $\phi$  and  $\varphi$ . The former is determined by the initial conditions while the latter depends on the natural frequency, the driving frequency and the damping.) The particular solution  $x_p(t)$  in Eq. (13.7) exhibits the expected resonance behavior. However, note that we have to be a little careful when we specify the location of the resonances. We obtain a slightly different answer if we

think of  $B$  as a function of  $\omega_D$  with  $\omega_0$  fixed, or the inverse. Here we focus on the former and learn that, thought of as an analytic function of the (possibly) complex frequency  $\omega_D$ , there are poles at the complex points  $i\lambda \pm \sqrt{\omega_0^2 - \lambda^2} = i\lambda \pm \omega_\lambda$ . The amplitude at the peak as probed with a real, physical frequency is given by

$$|B_{MAX}|(\omega_D = \omega_\lambda) = \frac{f}{2m\lambda\sqrt{\omega_0^2 - 3/4\lambda^2}}. \quad (13.8)$$

The magnitude at the peak value diverges as the damping goes away,  $\gamma, \lambda \rightarrow 0$ . The “Breit-Wigner” (or Lorentzian) shape of the dependence on the driving frequency is indicated in the figure. While the height of the peak scales like  $1/\lambda$  ( $\lambda \ll \omega_0$ ), the width scales like  $\lambda$ . This is because, as noted above, the magnitude of the amplitude  $B$  as a function of  $\omega_D$  has poles in the complex plane that are separated from the real axis by a distance that is proportional to the damping  $\lambda$ . (Note that as a function of  $\omega_D$  the “resonance” is not symmetric about the peak.)



Finally we can connect this discussion to the last lecture and consider a damped, driven, *nonlinear* oscillator (where linear superposition no longer applies but we will still consider a single driving frequency),

$$\ddot{x} + 2\lambda\dot{x} + \omega_0^2 x(1 + \alpha x^2) = \frac{f}{m} \cos(\omega_D t). \quad (13.9)$$

Let us focus first on a small nonlinear term, where we saw that the natural frequency is shifted by an amplitude dependent term (note that  $k$  is not the spring constant here – sorry about that),

$$\omega_\tau = \omega_0 \sqrt{1 + 3\alpha A^2/4} \approx \omega_0 (1 + 3\alpha A^2/8) \equiv \omega_0 (1 + kA^2). \quad (13.10)$$

So, at least approximately, we expect in this case that the following expression describes the square of the amplitude of the particular solution (recall that the homogeneous solution damps out)

$$|B|^2 \approx \frac{f^2}{m^2} \frac{1}{\left(\omega_0^2(1+k|B|^2) - \omega_D^2\right)^2 + 4\omega_D^2\lambda^2}. \quad (13.11)$$

We proceed by assuming that we are near the resonant frequency,  $\omega_D = \omega_0(1 + \delta)$ , and simplify using  $\delta \ll 1$ ,  $\lambda \ll \omega_0$ ,  $k|B|^2 \ll 1$

$$\begin{aligned} |B|^2 &\approx \frac{f^2}{m^2} \frac{1}{4\omega_0^4} \frac{1}{\left(k|B|^2 - \delta\right)^2 + \left(\frac{\lambda}{\omega_0}\right)^2} \\ \Rightarrow |B|^2 \left[ \left(k|B|^2 - \delta\right)^2 + \left(\frac{\lambda}{\omega_0}\right)^2 \right] &= \frac{f^2}{4m^2\omega_0^4}. \end{aligned} \quad (13.12)$$

This expression is numerically accurate only for small nonlinearities (small amplitudes) and near the resonance. However, it will teach us some qualitative lessons and we will use it for now even outside of the region of accuracy. In particular, considered as an equation for the magnitude of the amplitude of the particular solution, we notice that it is a cubic equation (for  $|B|^2$ ) with, in general, 3 solutions. On the other hand we are only interested in real solutions ( $|B|^2$  is real!) of the cubic equation and only one of the solutions is typically real for a given set of values for the parameters, *e.g.*, at any given value of  $\delta$ . We can obtain some sense of the expected behavior of the solutions of this equation by taking the derivative of  $|B|^2$  with respect to  $\delta$ . We find

$$\begin{aligned} \frac{d|B|^2}{d\delta} \left[ 3k^2|B|^4 - 4\delta k|B|^2 + \delta^2 + \left(\frac{\lambda}{\omega_0}\right)^2 \right] + 2\delta|B|^2 - 2k|B|^4 &= 0 \\ \Rightarrow \frac{d|B|^2}{d\delta} &= 2 \frac{|B|^2(k|B|^2 - \delta)}{3k^2|B|^4 - 4\delta k|B|^2 + \delta^2 + \left(\frac{\lambda}{\omega_0}\right)^2} \\ &= 2 \frac{|B|^4(k|B|^2 - \delta)}{\frac{f^2}{4m^2\omega_0^4} + 2k|B|^4(k|B|^2 - \delta)}. \end{aligned} \quad (13.13)$$

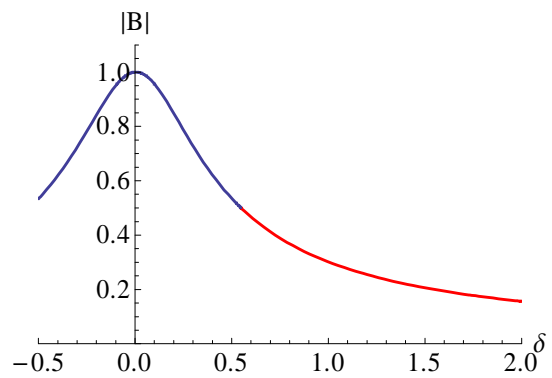
While these are messy expressions, Eqs. (13.12) and (13.13) do tell us an interesting story, which we now try to qualitatively understand. We want to be thinking about the response of the oscillator as we scan the frequency of the driving term near the natural frequency (*i.e.*, we vary  $\delta$ ) for a variety of strengths of the nonlinear terms (*i.e.*, values of  $\alpha$ ).

1) For a very small driving force with a small amplitude and/or for a small value of  $\alpha$  the nonlinearity is also very small ( $k|B|^2 \ll \delta$  except right at  $\delta = 0$ ) and, as a function of  $\delta$ , we have essentially a Breit-Wigner form (except right at the origin),

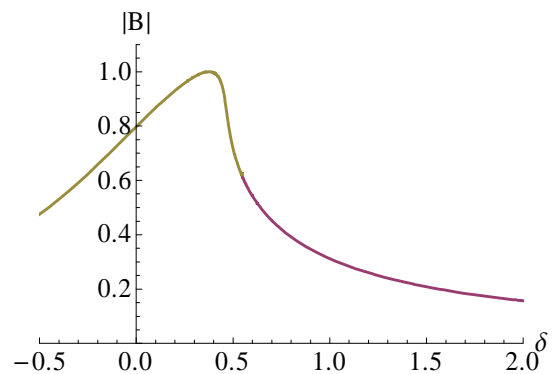
$$|B|^2 \approx \frac{f^2}{4\omega_0^4 m^2} \frac{1}{\delta^2 + \left(\frac{\lambda}{\omega_0}\right)^2}. \quad (13.14)$$

This is illustrated in the next figure (to be compared to the previous one but here plotted versus  $\delta = (\omega_D - \omega_0)/\omega_0$ ) corresponding to the parameters values  $\alpha = 0.01$  ( $k = 0.03/8$ ),

$(\lambda/\omega_0)^2 = 0.1$  and  $f^2/4m^2\omega_0^4 = 0.1$ . (The constraint of keeping only the real solution of the true cubic equation leads to a switching of solutions at  $(\omega - \omega_0)/\omega_0 \approx 0.55$ ; look at the color version of the figure.) Note from Eq. (13.13) that in this case we do expect a peak, *i.e.*, a vanishing derivative, near the origin.

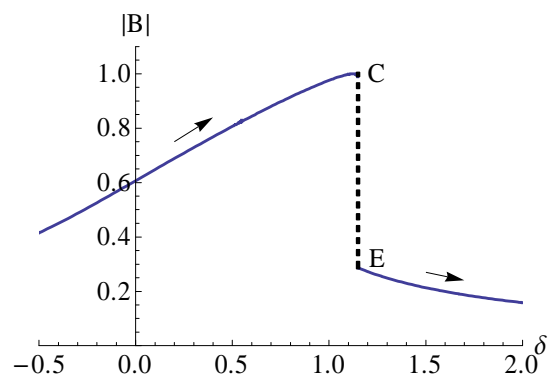
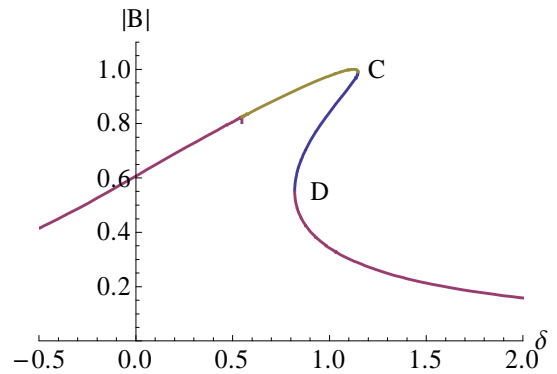


2) As we increase the strength of the nonlinearity (*i.e.*, increase  $\alpha$ , *i.e.*,  $k$ ) the shape of the distribution changes and the cubic behavior becomes more apparent. A similar change, along with an increase in the magnitude, occurs if we simply increase the strength of the driving force. Note in particular that the derivative will eventually develop a divergence (*i.e.*, the denominator in Eq. (13.13) vanishes), corresponding to a vertical region in the curve (near  $\delta \sim 0.5$ ) where the amplitude changes *discontinuously* with the

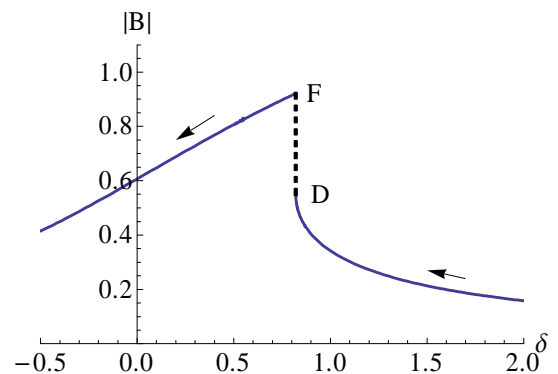


frequency. The figure here corresponds to  $\alpha = 1, k = 3/8, \lambda^2 = 0.1$  and  $f^2/4m^2\omega_0^4 = 0.1$ , and again there is a switch between solutions (still at about  $(\omega - \omega_0)/\omega_0 \approx 0.55$  where it is now clear that the derivative is nearly singular).

3) As we further increase  $\alpha$  eventually the fully cubic nature of the solution becomes apparent, *i.e.*, the dependence of  $|B|$  on  $\delta$  is clearly *triple-valued* in a range of  $\delta$ . This is illustrated in the next figure corresponding to  $\alpha = 3, k = 9/8, \lambda^2 = 0.1$  and  $f^2/4m^2\omega_0^4 = 0.1$  (recall again that we are intentionally keeping results when  $k|B|^2 \ll 1$  is not satisfied). As is evident from this plot, the derivative is divergent at 2 points (the points C and D in the figure), *i.e.*, the curve is vertical at two points. It is at these singular points that we switch from one solution to the next in order to use only the real solution of the cubic equation, *i.e.*, each of the 3 solutions is the appropriate real solution somewhere along this curve with the singular points (and the point near 0.55) serving to separate the various regions. Of course, the response of the system that we will see in practice, *i.e.*  $|B|$  versus  $\delta$ , will not look like this (upper) figure (even if our analysis were numerically correct). Consider approaching the singular region from below (by slowly increasing  $\delta$ ) as indicated in the figure to the right. At point C the amplitude of the system will not move “back under the cliff”. Rather the amplitude of the oscillation will drop discontinuously (falls off the cliff) to the lower curve indicated by the point E.

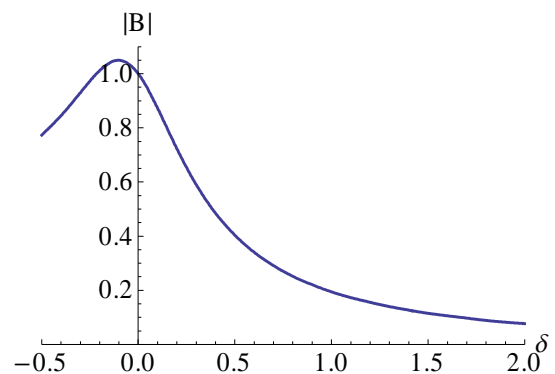


On the other hand, if we approach the singular region from frequencies above  $\omega_0$  (decreasing  $\delta$ ), the system will exhibit behavior more similar to that indicated in the next figure. It follows the previous full curve past the point E until the point D is reached, when the amplitude will jump discontinuously up to the upper branch of the curve at the point F.



The fact that the last two figures are not identical is an indication that such a nonlinear system will exhibit hysteresis, *i.e.*, the behavior of the system in the singular region depends on the direction with which this region is approached. It is a challenge to illustrate this behavior in a numerical simulation, but we will present here some results obtained using NDSolve in *Mathematica*. If we integrate for a long enough time, the homogeneous solution will damp out, and we will be able to see the particular solution. We can obtain the magnitude of the amplitude of the final stable motion by averaging the square of the amplitude over a fixed interval and multiplying by 2. In the singular region discussed above (where the nonlinearity is large), the amplitude  $|B|$  of this final behavior will depend on the initial conditions.

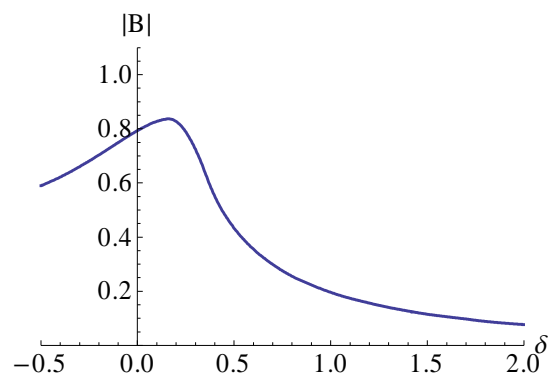
To simulate this effect we solve for the behavior of the system numerically and iteratively. As we slowly increase (or decrease) the driving frequency, we can use the result for the amplitude (at a fixed time) at the previous frequency as the initial condition at the new frequency. In this way the simulation is like the physical process of slowly increasing the frequency while the physical system is actually oscillating. The result of using the *Mathematica* code available on our web page is shown in the next figures. For the first conditions in 1) above,  $\alpha = 0.01$  ( $k = 0.03/8$ ),



$(\lambda/\omega_0)^2 = 0.1$  and  $f^2/4m^2\omega_0^4 = 0.1$ , the

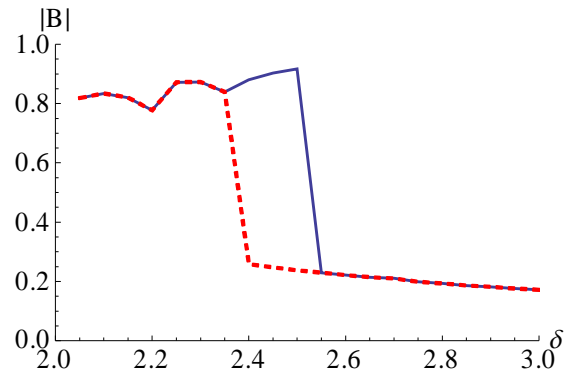
numerical results lead to the figure just above, which is quite similar to the approximate results above.

For the second set of parameter values,  $\alpha = 1$ ,  $k = 3/8$ ,  $\lambda^2 = 0.1$  and  $f^2/4m^2\omega_0^4 = 0.1$ , we numerically find the results in the next figure. These are similar to but far from identical to the approximate results above. In particular, we are approaching the singular (vertical) behavior more slowly in the full numerical results.



To obtain reasonably stable results in the singular region we look at a quite large value of  $\alpha$  and focus only on  $\delta$  values in the singular region. The values used are  $\alpha = 20$ ,  $k = 15/2$ ,  $\lambda^2 = 0.1$  and  $f^2/4m^2\omega_0^4 = 0.1$ , which results in the figure on the next page. The solid (blue) curve is for increasing driving frequency and the dashed

(red) is for decreasing frequency. There is clearly numerical noise but the hysteresis effect is clearly illustrated.



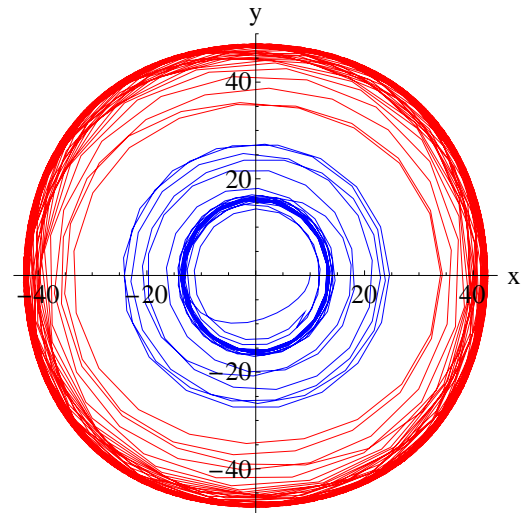
Now we turn to considering the 1-D driven, damped anharmonic oscillator as a flow problem in phase space. A useful way to perform this analysis is to think in terms of a 3-D phase space  $(x,y,z)$ , where the third dimension is the phase of the driving force ( $z = \omega_D t$ ). The flow equations (*i.e.*, Hamilton's equations) look like

$$\begin{aligned} \dot{x} &= y, \\ \dot{y} &= -2\lambda y - \omega_0^2 x(1 + \alpha x^2) + \frac{f}{m} \cos(z), \\ \dot{z} &= \omega_D. \end{aligned} \tag{13.15}$$

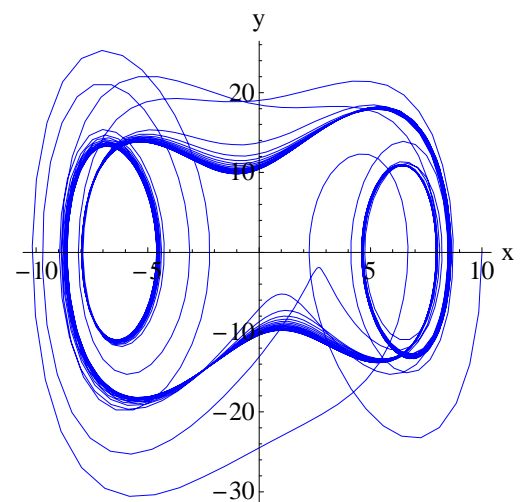
Our usual 2-D phase portraits correspond to projecting the motion in 3-D onto the  $(x, y)$  plane. As we will see, taking "snapshots" of the motion at fixed, regular intervals along the  $z$  axis is also a useful way to study the motion (called Poincaré sections). Compared to the elliptic and hyperbolic trajectories in phase space that we observed for the undamped and undriven, but anharmonic potentials in the previous lecture, the addition of damping and driving terms allows a much richer set of possible behaviors. In the case where the nonlinear terms are irrelevant we know that, independent of the initial conditions, the damping will push the solution to the trajectory corresponding to the familiar particular solution of Eq. (13.6). This will appear in phase space as an elliptic trajectory to which all initial trajectories, which do depend on the initial conditions, flow as time progresses, *i.e.*, energy is either added (by the driving force) or removed (by the damping) until the behavior is described by the particular solution. This stable large time behavior is called an attractor to denote the fact that in phase space it "attracts" the other initial trajectories. When we include the effects of nonlinearities several new features arise. The attractor trajectories can be much more complex than simple ellipses. Also there can be more than one attractor corresponding to the same system properties and the final attractor (particular solution) to which the system flows will depend on the initial conditions. The region in phase that separates the "basins of attraction" of 2 such attractors is labeled as the separatrix.

To illustrate some of these points consider first the behavior of the oscillator in a region of parameter space where the nonlinear parameter is not large, but the driving

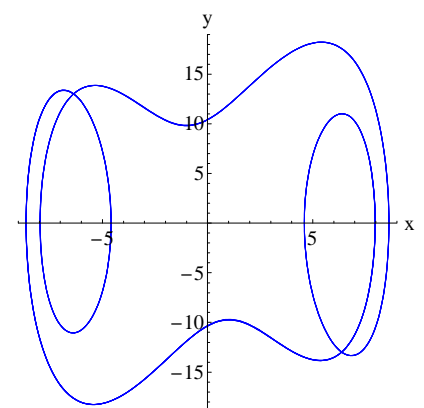
force is strong so that the resulting amplitude is fairly large. While we are not in the region of nearly discontinuous changes as above, there is still a strong dependence on (memory of) the initial conditions. For example, in the next figure we take  $\omega_0 = 1$ ,  $\omega_D = 1.18$ ,  $\alpha = 0.003$ ,  $2\lambda = 0.1$ ,  $f/m = 5$  and look at 2 different starting values for  $x(0)$  with  $y(0) = 0$ . Small (less than about 36) starting amplitudes yield small particular amplitudes ( $|B| \approx 15$ , the blue curves if you are reading in color), while large starting amplitudes yield large particular amplitudes ( $|B| \approx 40$ , the red curves). The corresponding 2 curves (the thick circles in the figure to the right) correspond to the corresponding 1-D attractors (lines), *i.e.*, a phase space trajectory that starts nearby one of the attractors will eventually flow to the nearest attractor path. This is illustrated in the (composite) phase portrait from the *Mathematica* code corresponding to the 2 different initial conditions. The regions of low line density is where the 2 different trajectories are slowly flowing to the final attractor trajectories where the density of lines is high. The blank region or separation between the 2 basins of attraction is called the separatrix (as noted above) and, in this case, is a circle at about radius 36.



The phase space trajectory becomes more complicated if we increase both the nonlinearity parameter and the strength of the force. We next choose parameter values of  $\alpha = 0.3$ ,  $2\lambda = 0.5$ ,  $f/m = 100$  with  $\omega_D = 4\omega_0/3$  and  $\omega_0 = 1$ . In this case the phase space trajectory looks like the substantially more complicated figure at the right.



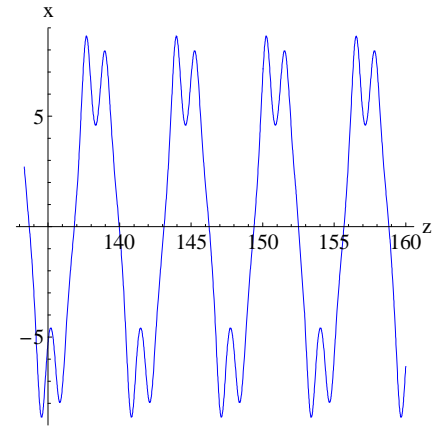
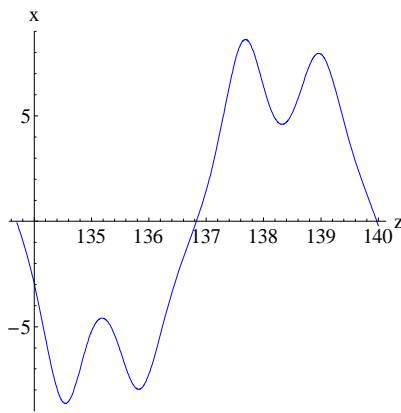
Although this looks complicated, if we look at late times, after the effects of the initial conditions have damped out, we still observe that the motion has settled down to (complicated, but) periodic behavior, *i.e.*, to the nearest attractor (or particular solution). The corresponding attractor is indicated in the figure to the right, which is just the same plot as the earlier one except that it shows only late times. The



frequency (and period) of this periodic motion is, as expected, the frequency of the driving force,  $\omega_D$ .

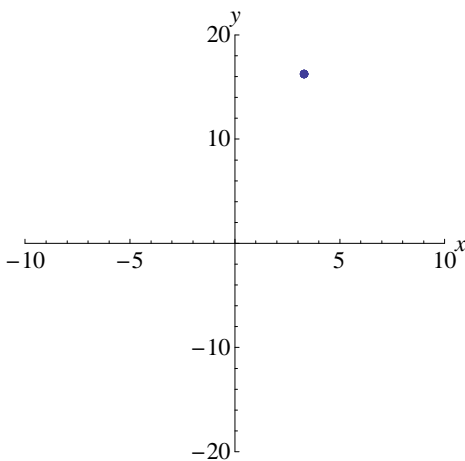
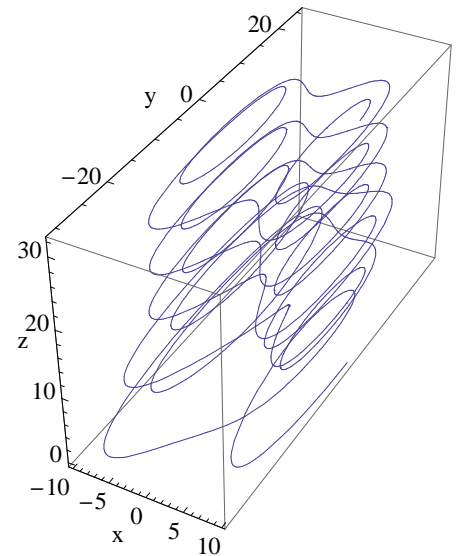
Identifying such periodic behavior is an important goal and we can pursue this goal in a couple of ways.

Consider first a plot of  $x$  versus  $z$  (the phase of the driving function which is proportional to time) for large values of  $z$ , yielding the figure at the right.



A careful look indicates a single period of the motion is as indicated in the figure to the left. The period in  $z$  is the expected  $2\pi$ .

Another way to look at this motion, which will be useful later, is to go back to full 3-D phase space  $(x, y = \dot{x}, z = \omega_D t)$  (you could think of this as 4-D phase space with a  $\dot{z}$  direction, but  $\dot{z} = \text{a constant}$  in this problem). The 3-D motion looks as in the figure to the right.

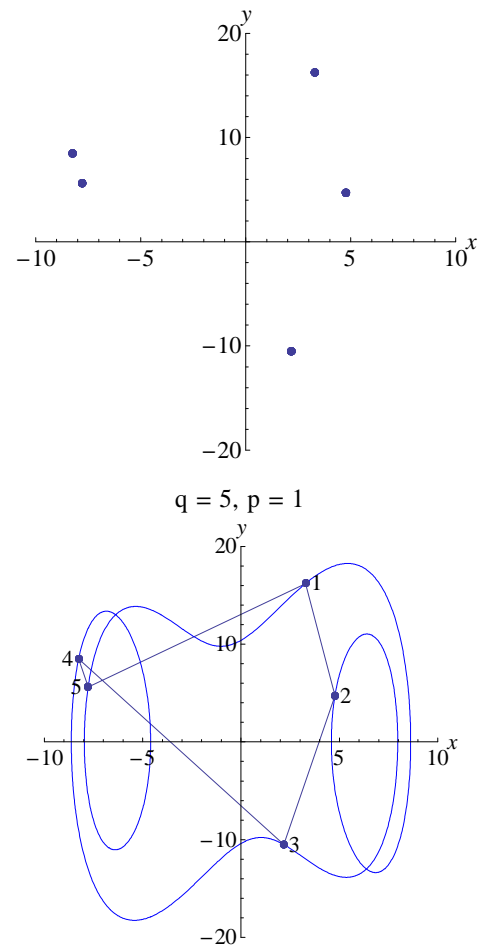


This is pretty messy but, as mentioned earlier, we can simplify the analysis by taking “snapshots” of the  $(x, y)$  plane at regular intervals in  $z$ , *i.e.*, take  $(x, y)$  slices at regular  $z$  values, say  $z = 2n\pi$ . If the motion is periodic and we synchronize the timing of the slices (at large times), the trajectory in  $(x, y, z)$  space will intersect the slices at the same point on each slice. When we

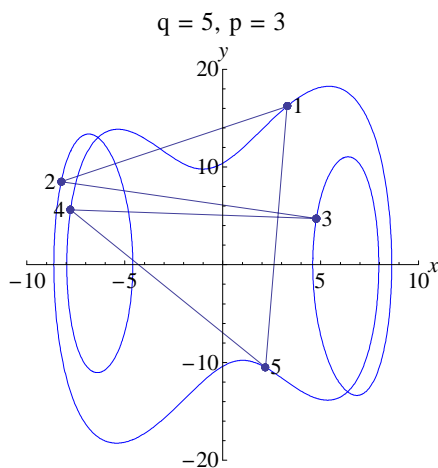
superimpose all the slices we get the Poincaré section. For example, the Poincaré section for our example is illustrated at the bottom of the previous page (10 slices starting at  $z = 200$  and spaced by  $2\pi$  in  $z$ ) – note that in this case the section contains just a single point.

The frequency with which we take the slices in  $z$  is called the strobe frequency,  $\omega_s$ , by B&G in Chapter 2. Here we have taken  $\omega_s = \omega_D$ . If we call the frequency of the periodic motion in the  $(x, y)$  plane  $\omega_{xy}$  (called  $\omega_0$  in B&G), then the behavior of the dots in the Poincaré section tells us about the ratio  $\omega_{xy}/\omega_s$ . In particular, if this ratio is a rational number,  $\omega_{xy}/\omega_s = p/q$  ( $p$  and  $q$  integer), then  $q$  is the number of points in the Poincaré section. The trajectory intersects the various slices only at these points, no matter how many slices we make. The order in which the points are visited is encoded in the integer  $p$ . After 1 point is visited, the next point to be visited is separated by  $[p - 1]$  points (see Fig 2.17 in B&G). So for our oscillator, where the frequency of the asymptotic behavior is just the driving frequency and we have chosen  $\omega_s = \omega_D$ , our Poincaré section above corresponds to the expected case  $p = q = 1$  (just one point).

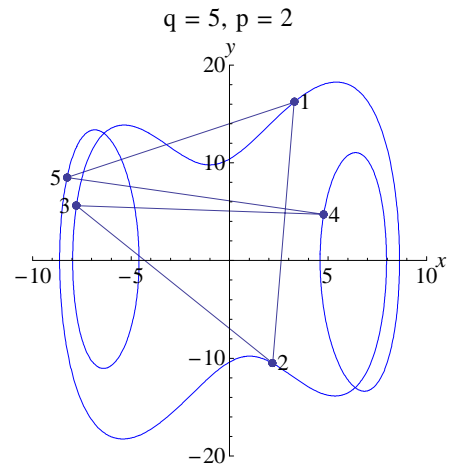
If instead we strobe at a frequency 5 times the driving frequency in the system above ( $q = 5, p = 1$ ), we find the Poincaré section shown to the right. Note that the specific location of the points depends on the specific value (phase) of  $z$  at the first slice. Changing this value without changing the strobe frequency moves the points around but does not change the number of points or the order in which they are visited. Changing the number of points, *i.e.*, changing  $\omega_s$ , without changing the initial  $z$  values, means that one of these points is the point in the figure above. To actually understand the ordering of the points we must recall the structure of the underlying attractor trajectory. The next figure superimposes the attractor, point labeling and connecting lines on the previous figure. As claimed for the case  $p = 1$  the points are visited in the order that they appear along the (complicated underlying attractor) trajectory.



To further illustrate the ordering issue considering strobing at the frequency  $\omega_s = 5\omega_D/2$ , ( $q = 5, p = 2$ ). The 5 points on the Poincaré section are the same but this time they are visited in alternating order (every other point) along the trajectory as indicated in the figure to the right. Next consider the case  $\omega_s = 5\omega_D/3$ , ( $q = 5, p = 3$ ),



which is like the previous Poincaré section except that 2 points are skipped between each visit, corresponding to the opposite order of visits from the previous case as indicated in the figure to the left. The last possibility,  $\omega_s = 5\omega_D/4$ , ( $q = 5, p = 4$ ), is like the initial 5 point case above ( $q = 5, p = 1$ ) but with the visits occurring in the opposite order.



In studies of actual systems we will usually “strobe” at the driving frequency. If the Poincaré section exhibits a fixed number of points at large times, the overall motion of the system is periodic. The ratio  $p/q$  plays much the same role as the winding number we defined in the case of the central force problem, a discussion we will return to briefly in the next lecture. It is perhaps surprising that, on the way to chaos,  $p/q$  can be nontrivial (*i.e.*, not just unity), because nonlinear systems can display responses not only at harmonics (integer multiples) of the driving frequencies,  $n\omega_D, n = 1, 2, 3, \dots$ , but also at subharmonics (integer fractions),  $\omega_D/n, n = 2, 3, \dots$ . This behavior is often called period doubling. As true chaotic behavior sets in the Poincaré section will contain a growing number of non-coincident points at large times, mapping out a complicated figure. Such motion is clearly aperiodic or quasiperiodic (corresponding to irrational values for  $p/q$ ), although a lack of overall periodicity is not, in itself, a guarantee of chaos (*i.e.*, it is necessary but not sufficient).

Before turning to explicit chaos in the case of the driven, damped oscillator we return briefly in the next lecture to further discussion of phase space flows and also return the central force problem.